Supporting Information

Cluster-Induced Aggregation in Polyurethane Derivatives with Multicolour Emission and Ultra-long Organic Room Temperature Phosphorescence

Nan Jiang [a], Ke-Xin Li [a], Jia-Jun Wang [a], Chen-Sen Li [b], Xiao-Yu Xu [a], Yan-Hong Xu [a,*], Martin R. Bryce [c,*]

[a] Key Laboratory of Preparation and Applications of Environmental Friendly Materials, Key Laboratory of Functional Materials Physics and Chemistry of the Ministry of Education (Jilin Normal University), Changchun, 130103, China.
[b] Department of Chemistry, Hong Kong Branch of Chinese National Engineering Research Center for Tissue Restoration and Reconstruction and Institute for Advanced Study, The Hong Kong University of Science and Technology Clear Water Bay, Kowloon, Hong Kong 999077, China
[c] Department of Chemistry, Durham University, Durham DH1 3LE, UK

*Corresponding authors. E-mail: xuyh198@163.com; m.r.bryce@durham.ac.uk

1. Experimental details

Materials

Materials obtained from commercial suppliers were used without further purification unless otherwise stated. All glassware, syringes, magnetic stirring bars, and needles were thoroughly dried in a convection oven.

Characterisation

The UV-vis absorption spectra were recorded on a Shimadzu UV-3100 spectrophotometer. The luminescence movie and photos were taken by an iPhone 14 pro under the irradiation of a hand-held UV lamp at room temperature. ^{1}H NMR spectra were recorded on a Varian 500 MHz spectrometer. The ^{1}H NMR spectra were referenced internally to the residual proton resonance in DMSO-d_6 (δ 2.5 ppm). The molecular weights of the polyurethane samples were determined by gel permeation chromatography (GPC) on a Waters 410 instrument with monodispersed polystyrene as the reference and THF as the eluent at 35°C. Scanning electron microscope (SEM) images were obtained using a JEOL model JSM-6700 instrument operating at an accelerating voltage of 5.0 kV. The samples were prepared by placing microdrops of the solution on a holey carbon copper grid. Steady-state photoluminescence/phosphorescence spectra and phosphorescence lifetime were measured using a Hitachi F-4700 instrument. The fluorescence lifetime and photoluminescence quantum efficiency were obtained on an Edinburgh FLS-1000 instrument. The fluorescence microscope images were obtained using a ZEISS Scope.A1 with HBO 100. The ZEISS Scope.A1 was equipped with three fluorescence modules. When Ex=365 nm, Em collects light > 420 nm; when Ex=400-460 nm, Em=500-600 nm; when Ex=420-450 nm, Em collects light > 515 nm. WAXD data were obtained using an Empyrean instrument. Solution electrochemical measurements data were obtained using a CHI 660E Chenhua instrument.

Density functional theory (DFT) calculations

Density functional theory (DFT) calculations were all performed using the Gaussian 16 C.01 program[S1] at the B3LYP/6-31G(d) level. The DFT calculations were performed on the polyurethane with two repeating units.

Calculation of spin-orbit coupling (SOC)

By the means of DFT and TD-DFT, the ground state and excited state geometry of the studied molecules were optimised in Gaussian 16 program and the vibration frequencies were calculated. After the S_1 state was optimised using Gaussian 16, the spin-orbit coupling (SOC) constant between the S_1 and T_1 states was calculated using ORCA 5.0.3.[S2]

Molecular dynamics simulation calculation method

In Materials Studio (MS) the initial model of the molecule was constructed using the "Amorphous Cell" module, and the initial density was set to 1.0 g/cm³. Periodic boundary conditions were used, i.e., boxes were used in MS to represent the environment outside the molecule. 35 molecules were invested in the construction process, resulting in a total of 10 AC boxes. The structure was then subjected to 10,000 energy-minimisation iterations using the Smart algorithm to rule out unreasonable contact situations, such as overlapping parts and overly dense contact between molecules. In this step, the conformation with the lowest energy was selected as the starting point for the subsequent molecular dynamics simulation. Next, NPT dynamics simulations were used to obtain the physical properties of the system, such as density, volume, kinetic energy, and potential energy, resulting in the final equilibrium structure. NPT dynamics simulations were conducted at 298.15K for a total duration of 5 nanoseconds with 1 femtosecond per time

step, resulting in 50001 models.

In the simulation, the Dreiding force field was used to calculate the interatomic interactions within the system. The long-range electrostatic interaction terms were solved by the Ewald summation method with an accuracy of 0.001 kcal·mol⁻¹. The van der Waals interaction force was calculated using an atom-based method with a cut-off distance of 12.5 Å. At the same time, to control the system temperature, the Nose-Hoover thermostat and the Berendsen constant pressure were used to maintain the pressure stability. All molecular dynamics simulations were performed using a time step of 1 femtosecond. In summary, in this research process, the initial model was built using Amorphous Cell module in Materials Studio. Through steps such as energy minimisation and dynamic simulation, the balanced structure and physical properties of the system were obtained. The interaction was calculated using the Dreiding force field, with appropriate temperature and pressure control, providing strong support for further molecular modelling studies.[S3,S4]

Radial distribution function

The calculation equation for the radial distribution function (RDF) can be described as:[S5,S6]

$$g(r) = \lim_{dr \to 0} \frac{p(r)}{4\pi \left(\dfrac{N_{pairs}}{V} \right) r^2 dr}$$

where r is the distance between each atom pair, $g(r)$ is the radial distribution function, $p(r)$ is the average number of atom pairs. N_{pairs} is the total number of atom pairs, V is the volume of the simulation cell.

Synthesis of PUB

A mixture of cyclopropylboronic acid (0.675 g, 7.86 mmol), polyethylene glycol mono-methyl ether (M_w = 200 g mol⁻¹; 1.188 g, 5.94 mmol), anhydrous THF (10 mL), trimethylhexa-1,6-diyl diisocyanate (2.479 g, 10.83 mmol) and 1,4-diazabicyclooctane triethylenediamine (DABCO) (0.035 g, 0.315 mmol) was stirred in N₂ atmosphere at 68°C for 24 h until the clear solution became viscous, indicating that polymerisation had occurred. After cooling to room temperature, the mixture was added to excess *tert*-butyl methyl ether drop by drop for reverse precipitation to give a product which was then dried under vacuum at room temperature for 24 h to obtain polyurethane **PUB** (2.75 g, 63% yield). ¹H NMR (400 MHz, DMSO-d_6, δ [ppm]): 7.28 (s, 2H), 7.16 (s, 2H), 7.11 (s, 1H), 4.03 (s, 4H), 3.4-3.6 (broad, PEG protons), 3.23 (s, 6H; PEG terminal -OCH₃ protons), 2.6-3.1 (broad, 4H), 0.3-1.7 (broad, 25H). FT-IR: 3336 cm⁻¹ (N-H), 2871 cm⁻¹ and 2958 cm⁻¹ (-CH₂- asymmetric and symmetric stretch), 1709 (C=O), 1372 (B-O), 1103 cm⁻¹ (C-O-C stretch PEG). M_n=14063 g mol⁻¹, M_w=18422 g mol⁻¹, PD=1.31.

Synthesis of PUG

A mixture of cyclopropylboronic acid (0.675 g, 7.86 mmol), polyethylene glycol mono-methyl ether (M_w = 200 g mol⁻¹; 1.188 g, 5.94 mmol), anhydrous THF (3 mL), anhydrous DMSO (3 mL), trimethylhexa-1,6-diyl diisocyanate (2.479 g, 10.83 mmol) and 1,4-diazabicyclooctane triethylenediamine (DABCO) (0.035 g, 0.315 mmol) was stirred in N₂ atmosphere at 100°C for 48 h until the clear solution became viscous, indicating that polymerisation had occurred. After cooling to room temperature, the mixture was added to excess *tert*-butyl methyl ether drop by drop for reverse precipitation to give a product which was then dried under vacuum at room temperature for 24 h to obtain polyurethane **PUG** (2.475 g, 57% yield). ¹H NMR (400 MHz, DMSO-d_6, δ [ppm]): 7.28 (s, 2H), 7.16 (s, 2H), 7.11 (s, 1H), 4.03 (s, 4H), 3.4-3.6 (broad, PEG protons), 3.23 (s, 6H; PEG terminal -OCH₃ protons), 2.6-3.1 (broad, 4H), 0.3-1.7 (broad, 25H). FT-IR: 3422 cm⁻¹ (N-H), 2852 cm⁻¹ and 2951 cm⁻¹ (-CH₂- asymmetric and symmetric stretch), 1627 (C=O), 1383 (B-O), 1103 cm⁻¹ (C-O-C stretch PEG). M_n=15067 g mol⁻¹,

M_w=19626 g mol^{-1}, PD=1.30.

Synthesis of PUY

A mixture of cyclopropylboronic acid (0.675 g, 7.86 mmol), polyethylene glycol mono-methyl ether (M_w = 200 g mol^{-1}; 1.188 g, 5.94 mmol), anhydrous THF (2 mL), anhydrous DMSO (4 mL), trimethylhexa-1,6-diyl diisocyanate (2.479 g, 10.83 mmol) and 1,4-diazabicyclooctane triethylenediamine (DABCO) (0.035 g, 0.315 mmol) was stirred in N$_2$ atmosphere at 110°C for 48 h until the clear solution became viscous, indicating that polymerisation had occurred. After cooling to room temperature, the mixture was added to excess *tert*-butyl methyl ether drop by drop for reverse precipitation to give a product which was then dried under vacuum at room temperature for 24 h to obtain polyurethane **PUY** (2.562 g, 59% yield). ^{1}H NMR (400 MHz, DMSO-d_6, δ [ppm]): 5.90 (s, 2H), 5.72 (s, 2H), 4.03 (s, 4H), 3.4-3.6 (broad, PEG protons), 3.23 (s, 6H; PEG terminal -OCH$_3$ protons), 2.6-3.1 (broad, 4H), 0.3-1.7 (broad, 25H). FT-IR: 3410 cm^{-1} (N-H), 2873 cm^{-1} and 2937 cm^{-1} (-CH$_2$- asymmetric and symmetric stretch), 1632 (C=O), 1294 (B-O), 1032 cm^{-1} (C-O-C stretch PEG). M_n=15585 g mol^{-1}, M_w=24845 g mol^{-1}, PD=1.59.

Synthesis of PUR

A mixture of cyclopropylboronic acid (0.675 g, 7.86 mmol), polyethylene glycol mono-methyl ether (M_w = 200 g mol^{-1}; 1.188 g, 5.94 mmol), anhydrous DMSO (6 mL), trimethylhexa-1,6-diyl diisocyanate (2.479 g, 10.83 mmol) and 1,4-diazabicyclooctane triethylenediamine (DABCO) (0.035 g, 0.315 mmol) was stirred in N$_2$ atmosphere at 130°C for 48 h until the clear solution became viscous, indicating that polymerisation had occurred. After cooling to room temperature, the mixture was added to excess *tert*-butyl methyl ether drop by drop for reverse precipitation to give a product which was then dried under vacuum at room temperature for 24 h to obtain polyurethane **PUR** (2.61 g, 60% yield). ^{1}H NMR (400 MHz, DMSO-d_6, δ [ppm]): 6.57 (s, 3H), 6.31 (s, 1H), 4.03 (s, 4H), 3.4-3.6 (broad, PEG protons), 3.23 (s, 6H; PEG terminal -OCH$_3$ protons), 2.6-3.1 (broad, 4H), 0.3-1.7 (broad, 25H). FT-IR: 3329 cm^{-1} (N-H), 2880 cm^{-1} and 2935 cm^{-1} (-CH$_2$- asymmetric and symmetric stretch), 1681 (C=O), 1292 (B-O), 1037 cm^{-1} (C-O-C stretch PEG). M_n=11851 g mol^{-1}, M_w=15115 g mol^{-1}, PD=1.27.

The preparation of information transmission models

Another polyurethane derivative **PUC** was synthesised by reacting the raw material at 90°C for 48 h. **PUC** has the same chemical structure as the other PUs (Fig. S4c) and similar fluorescence to **PUY**. **PUC** had M_n 15227 g mol^{-1} measured by GPC. The substrate for the images was a black paperboard for drawing and the PU powders were stuck onto it with double-sided tape.

The M_n of **PUC** (15227) is very close to that of **PUY** (15585) measured by GPC. Therefore, the fluorescence colour of **PUC** is like that of **PUY**. However, relative to molecular weight and chemical structure, for NCLPs, the aggregation structure ultimately plays a decisive role in the material's photophysical properties. The microstructure of **PUC** powder was obtained under the same conditions as the other PUs. Although **PUC** is partially clustered (Fig. S4b) it does not form a super-cluster structure that is seen for **PUY**. This could be the reason why **PUC** does not show RTP.
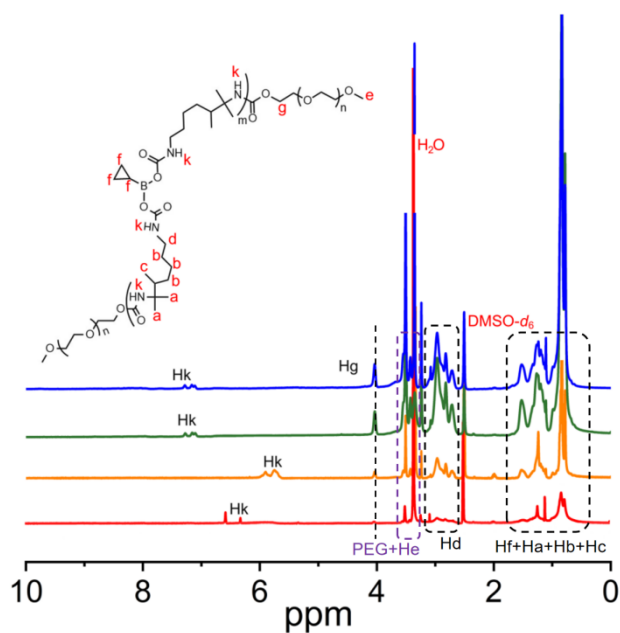
2. Structural characterisation

Fig. S1 ^{1}H NMR spectra in DMSO-d_6: from top to bottom **PUB**, **PUG**, **PUY**, **PUR**.
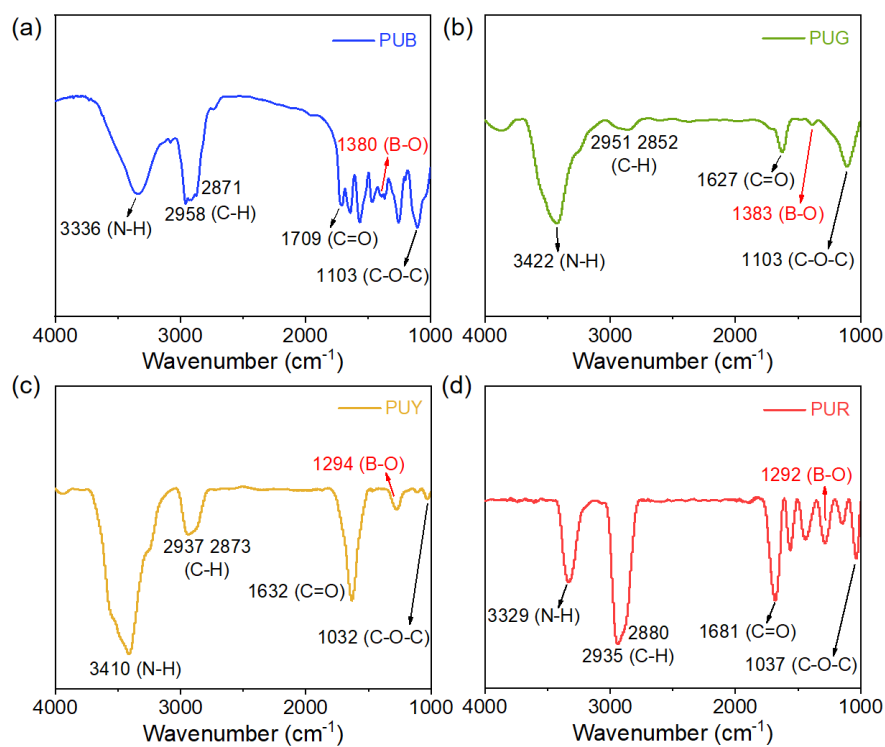

Fig. S2 FT-IR spectra of (a) **PUB**, (b) **PUG**, (c) **PUY** and (d) **PUR** in the solid state.
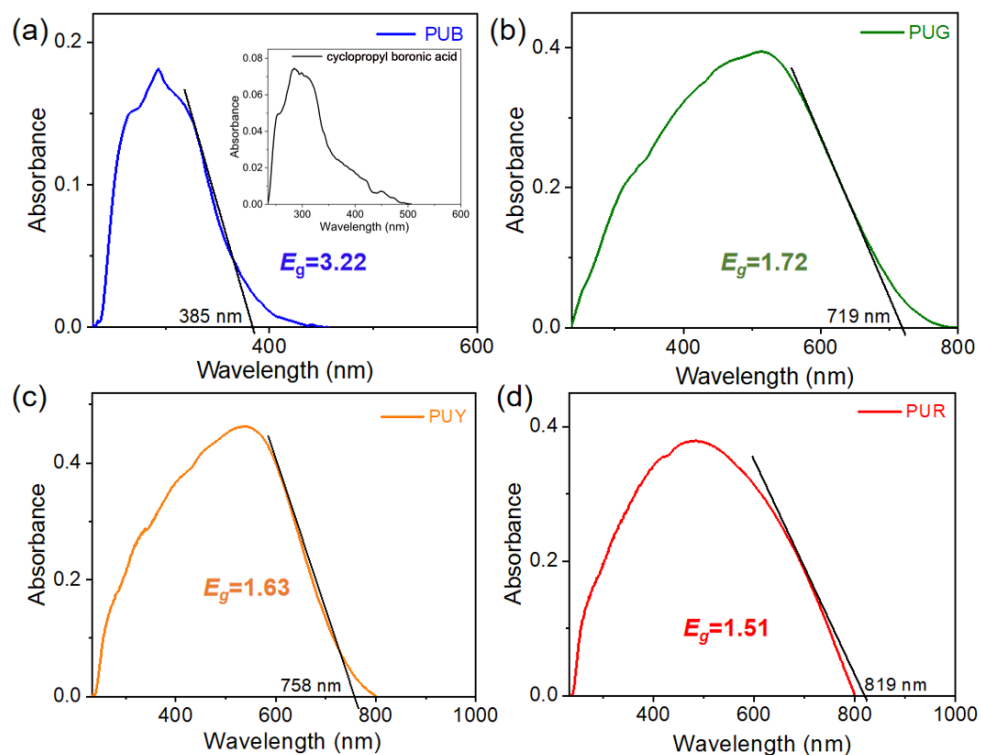
3. Photophysical properties

Fig. S3 UV-vis spectra of (a) **PUB**; Insert: cyclopropyl boronic acid monomer (b) **PUG**; (c) **PUY**; (d) **PUR** in the solid state.
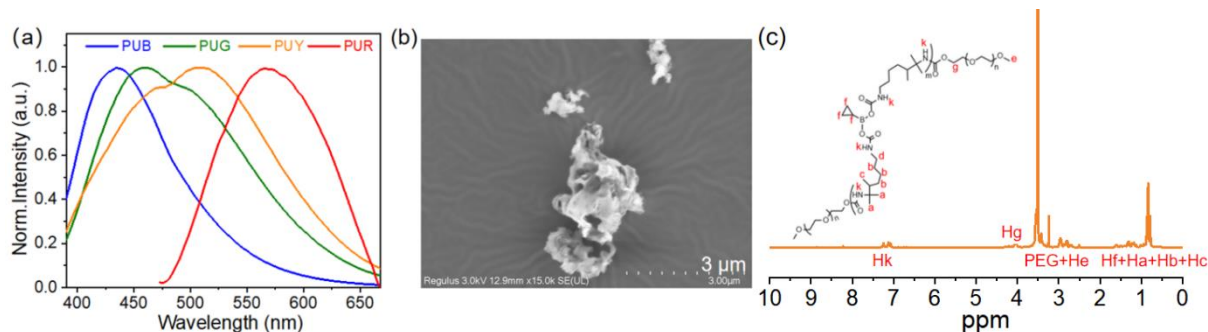

Fig. S4 (a) Fluorescence spectra of **PUB**, **PUG**, **PUY** and **PUR** powders at 365 nm excitation. (b) The SEM image of **PUC** in ethanol (20 mg mL^{-1}). (c) ^{1}H NMR spectra in DMSO-d_6 of **PUC**.
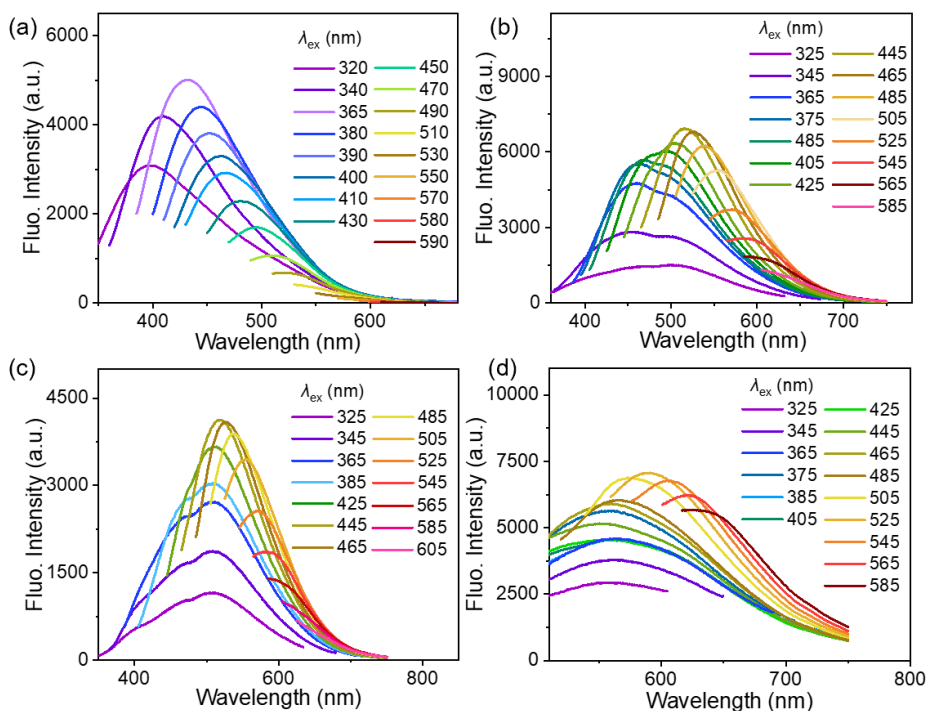
Fig. S5 Fluorescence spectra of (a) **PUB**, (b) **PUG**, (c) **PUY** and (d) **PUR** powders at varying λ_{ex}.
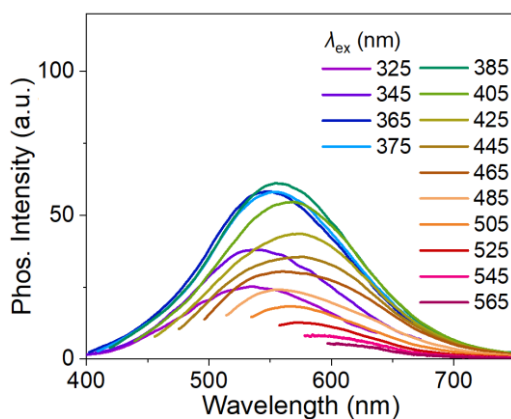
Fig. S6 Phosphorescence spectra of **PUY** powder at varying λ_{ex}.
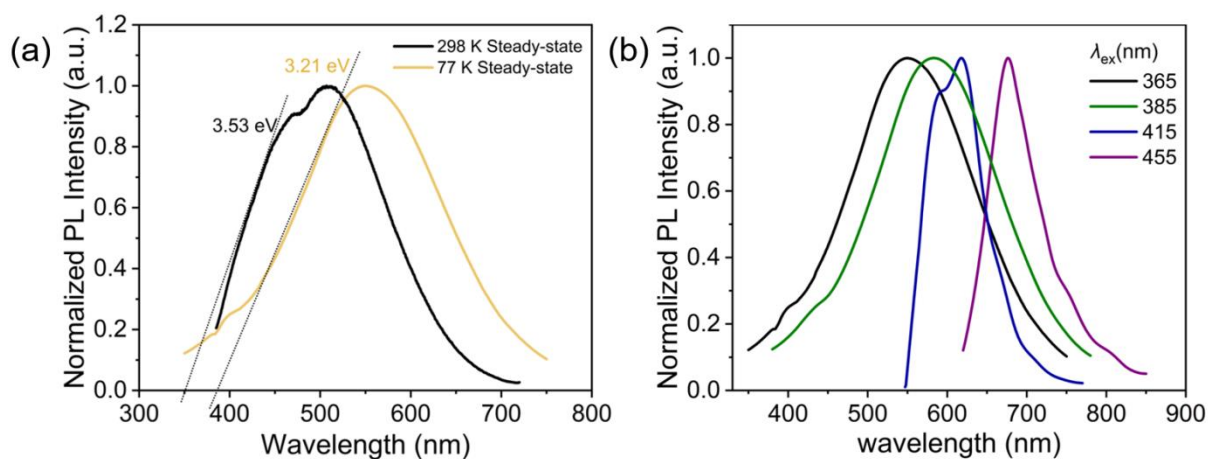
Fig. S7 (a) Steady-state and transient-state emission spectra in the powder state and corresponding excited energy levels of S_1 and T_1 states of **PUY**. (b) PL spectra of **PUY** at 77 K at varying λ_{ex}.
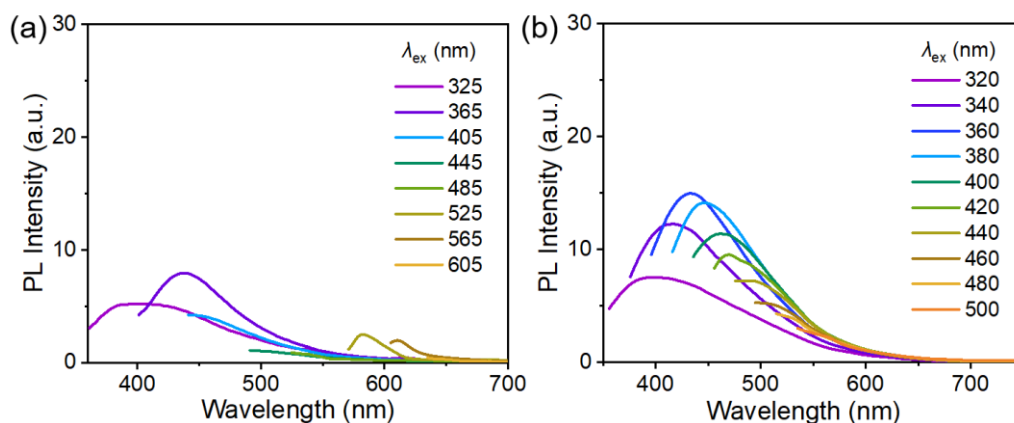
Fig. S8 Fluorescence spectra of (a) catalyst DABCO (b) Cyclopropylboronic acid monomer powders at varying λ_{ex}.
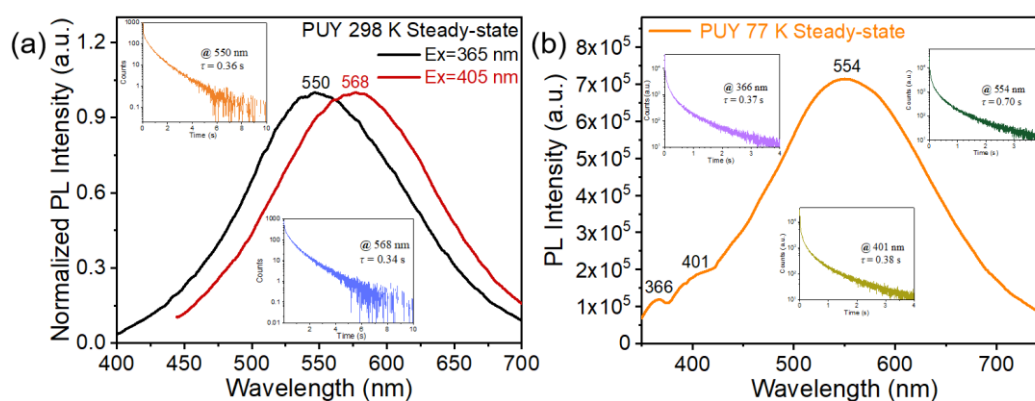
Fig. S9 (a) Normalised PL spectra of **PUY** at 298 K at varying λ_{ex}. Insert: Lifetime measured at different peak positions. (b) PL spectra of **PUY** at 77 K. Insert: Lifetime measured at different peak positions.
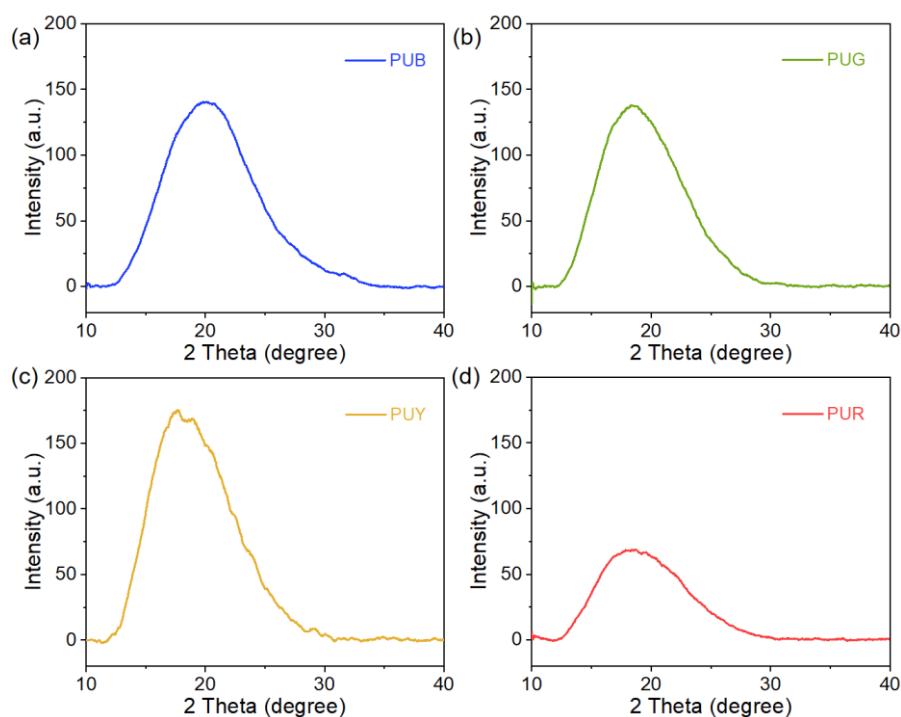

Fig. S10 XRD patterns of (a) **PUB**, (b) **PUG**, (c) **PUY** and (d) **PUR** powders.
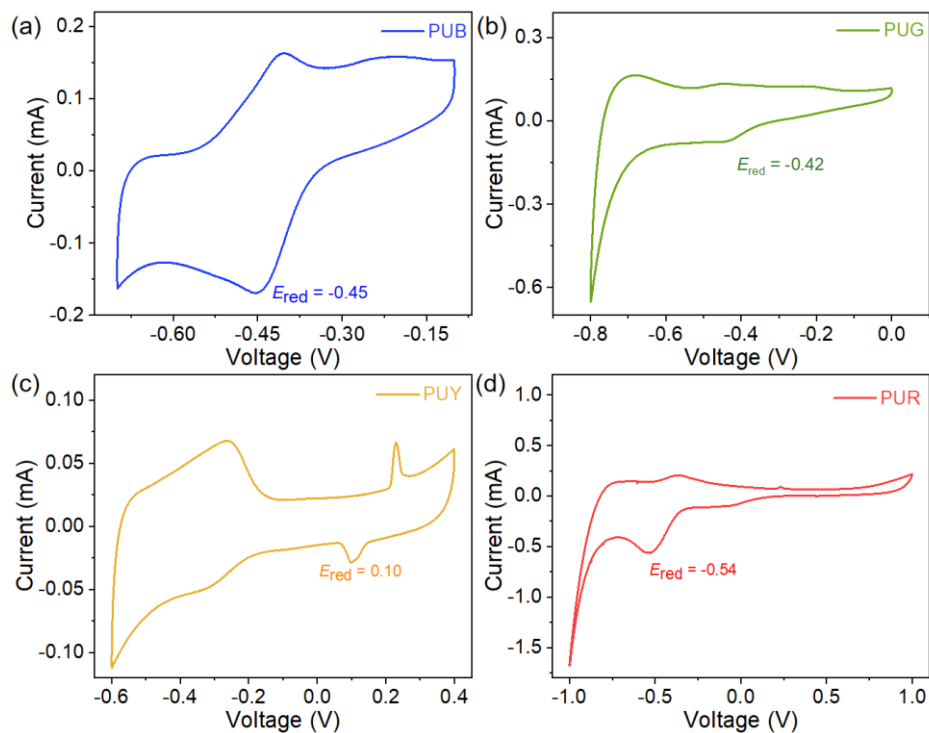
4. Electrochemical properties

Fig. S11 Cyclic voltammetry plots of **PUB**, **PUG**, **PUY**, and **PUR**, Fc (ferrocene) as external standard, 0.1 M Na_2CO_3 as electrolyte, scan rate 100 mV s^{-1}.
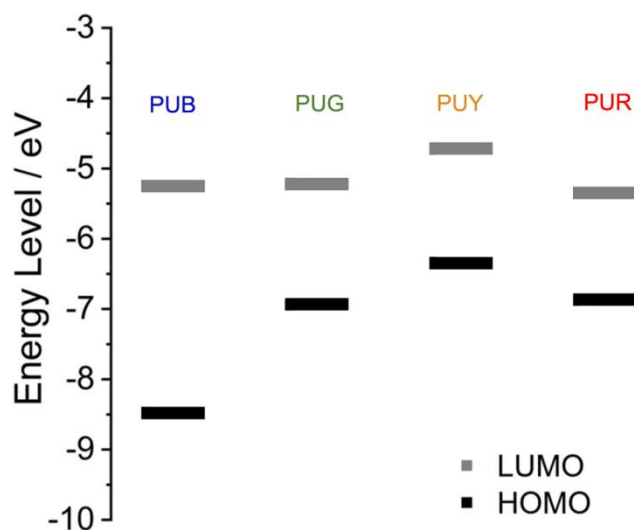

Fig. S12 Comparison of the experimentally determined energy levels of **PUB**, **PUG**, **PUY**, and **PUR**. LUMO levels are determined as $E=-(4.8+E_{red})$ eV and HOMO levels as $E_{HOMO}=E_{LUMO}-E_g$ using energy gaps (E_g) from UV-vis spectroscopy according to the equation $E_g = 1240/\lambda_{abs}$.

5. Molecular dynamics simulations
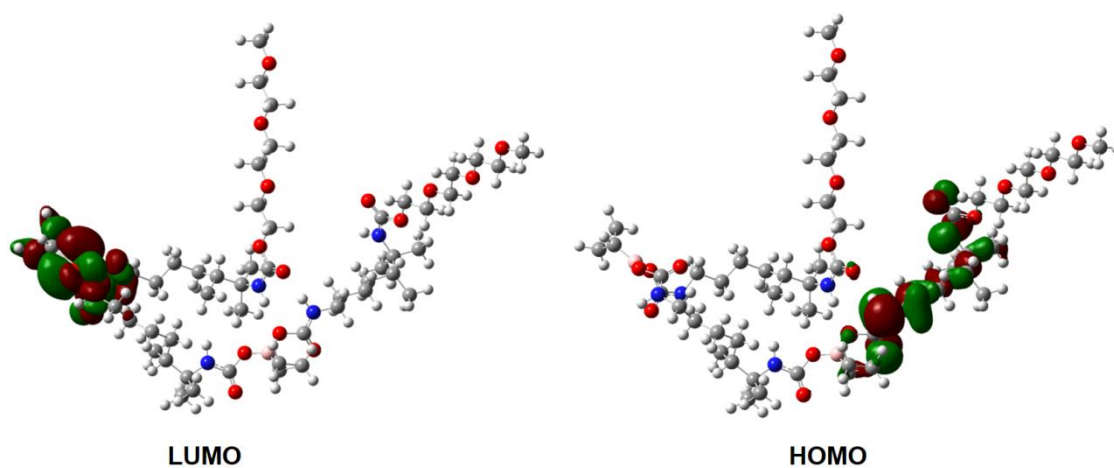

LUMO　　　**HOMO**
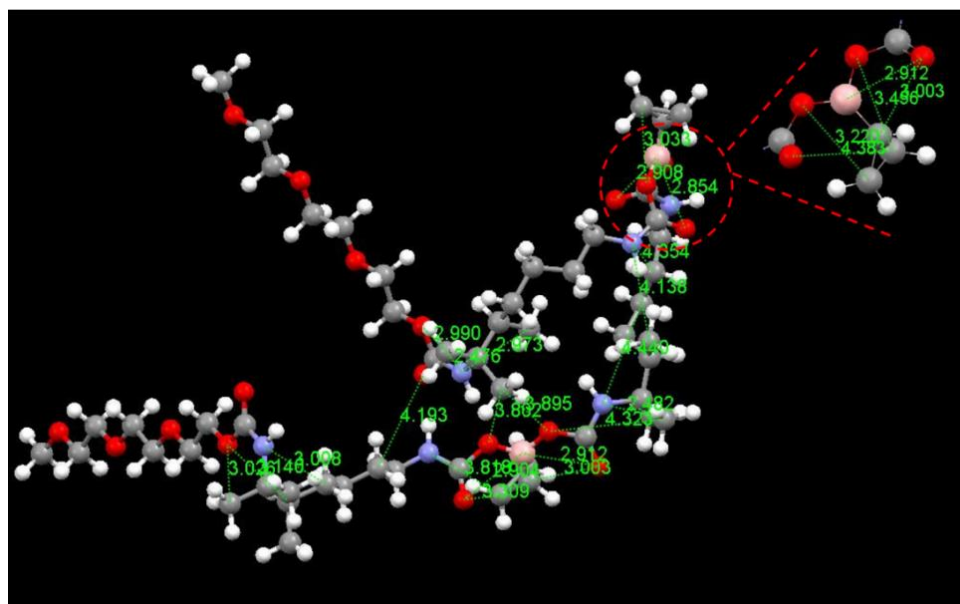
Fig. S13 HOMO-LUMO orbital diagram of the PUs.

Fig. S14 Diagram of short contacts, hydrogen-bonding interactions and through-space dative bonds within the PU chain. (C – gray; H – white; N – blue; O – red; B – pink).
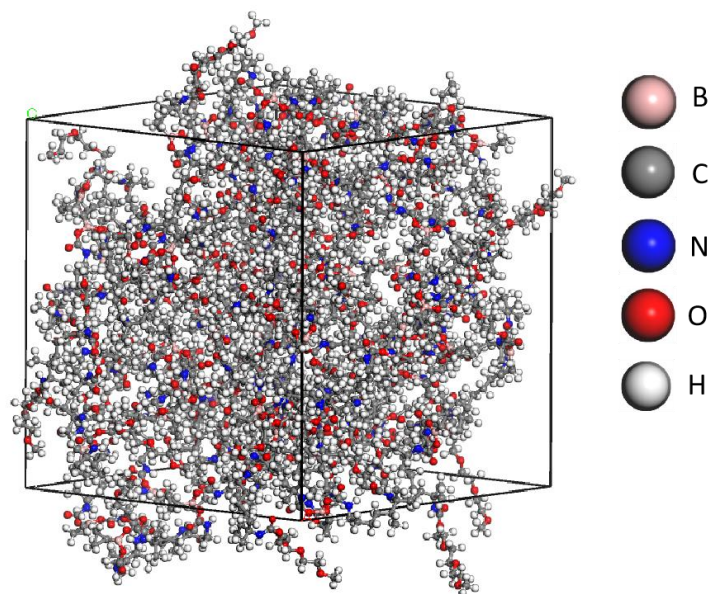
Fig. S15 Snapshot of the simulation box of the PU system at 5 ns last frame by molecular dynamics simulation.

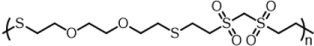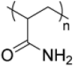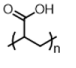**Table S1.** Phosphorescence wavelengths (λ_{em}) and lifetimes (τ) of pure NCLPs reported in the literature.
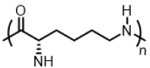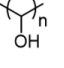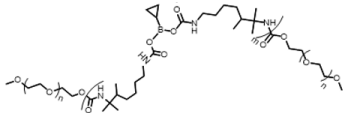
Molecular structure	λ_{em} (nm)	τ	References
	520	4.2 ms	*Macromol. Rapid Commun.*, 2021, **42**, 2100036.
	480	98 ms	*Mater. Chem. Front.*, 2020, **4**, 1198.
	503	35.5 ms	*J. Phys. Chem. B*, 2020, **124**, 8928.
	489	117 ms	*Mater. Chem. Front.*, 2019, **3**, 257.
	484	207 ms	*ChemPhysChem.*, 2020, **21**, 36.
	438	89 ms	*Chin. Chem. Lett.*, 2023, **34**, 107684.
	603	450 ms	This work

Table S2. Molecular weight data of the PUs from GPC.

	PUB	PUG	PUY	PUR
M_n / g mol^{-1}	14063	15067	15585	11851
M_w / g mol^{-1}	18422	19626	24845	15115
M_P / g mol^{-1}	13769	15227	14239	8194
PDI	1.31	1.30	1.59	1.27

Table S3. The fluorescence quantum efficiency (QY) and luminescence lifetimes (LT) of the PUs.

	PUB	PUG	PUY	PUR
QY	2.6%	2.1%	3.3%	0.2%
	442 nm	**462 nm**	**508 nm**	**559 nm**
LT	4.43 ns	4.46 ns	4.68 ns	3.75 ns
			603 nm	
LT			0.45 s	

Table S4. Comparison of electrochemical data of the PUs.

	$E_g^{opt\ a}$ / eV	$E_{red}^{CV\ b}$ / V	$E_{HOMO}^{\ c}$ / eV	$E_{LUMO}^{\ c}$ / eV
PUB	3.22	0.45	-8.47	-5.25
PUG	1.72	0.42	-6.94	-5.22
PUY	1.63	0.29	-6.72	-5.09
PUR	1.51	0.06	-6.37	-4.86

[a] E_g^{opt} =1240/λ_{abs} (λ_{abs} was measured by UV-vis spectroscopy); [b] E_{red}^{CV} was estimated from the reduction peak onsets. [c] $E_{LUMO} = - (4.8+E_{red})$, $E_{HOMO} = E_{LUMO} - E_g^{opt}$.

Table S5. Conformational parameters of optimised model of a single PU chain. (C – gray; H – white; N – blue; O – red; B – pink).
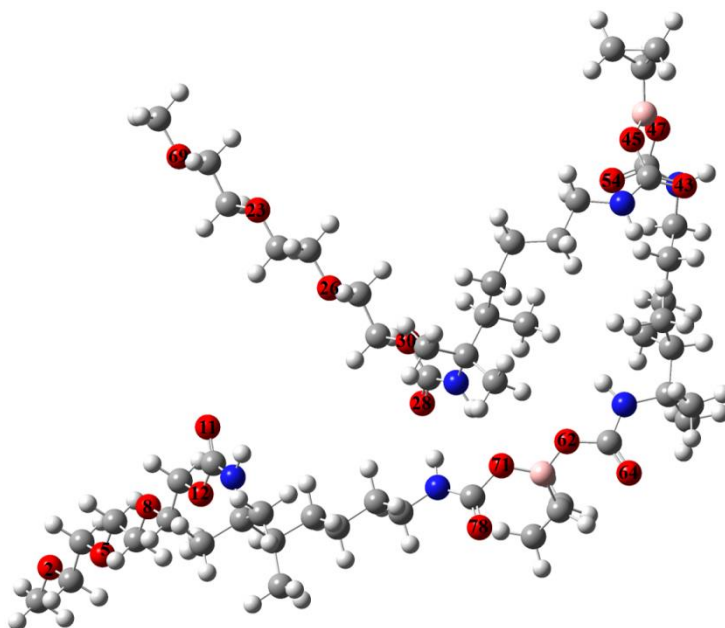
	Distance (Å)
O47-O54	2.28
O43-O45	2.28
O54-O45	3.04
O30-O28	2.27
O54-O43	3.50
O62-O64	2.29
O71-O62	2.29
O69-O23	3.59
O23-O26	3.59
O78-O71	2.29
O11-O12	2.28
O12-O8	3.59
O8-O5	3.59
O5-O2	3.59

Table S6. The calculated SOC coefficients.

$S_1{\rightarrow}T_1$	$S_1{\rightarrow}T_2$	$S_1{\rightarrow}T_3$
6.89024673 cm^{-1}	29.17801056 cm^{-1}	17.4355757 cm^{-1}

References

S1. Gaussian 16, Revision C.01, M. J. Frisch, G. W. Trucks, H. B. Schlegel, G. E. Scuseria, M. A. Robb, J. R. Cheeseman, G. Scalmani, V. Barone, G. A. Petersson, H. Nakatsuji, X. Li, M. Caricato, A. V. Marenich, J. Bloino, B. G. Janesko, R. Gomperts, B. Mennucci, H. P. Hratchian, J. V. Ortiz, A. F. Izmaylov, J. L. Sonnenberg, D. Williams-Young, F. Ding, F. Lipparini, F. Egidi, J. Goings, B. Peng, A. Petrone, T. Henderson, D. Ranasinghe, V. G. Zakrzewski, J. Gao, N. Rega, G. Zheng, W. Liang, M. Hada, M. Ehara, K. Toyota, R. Fukuda, J. Hasegawa, M. Ishida, T. Nakajima, Y. Honda, O. Kitao, H. Nakai, T. Vreven, K. Throssell, J. A. Montgomery, Jr., J. E. Peralta, F. Ogliaro, M. J. Bearpark, J. J. Heyd, E. N. Brothers, K. N. Kudin, V. N. Staroverov, T. A. Keith, R. Kobayashi, J. Normand, K. Raghavachari, A. P. Rendell, J. C. Burant, S. S. Iyengar, J. Tomasi, M. Cossi, J. M. Millam, M. Klene, C. Adamo, R. Cammi, J. W. Ochterski, R. L. Martin, K. Morokuma, O. Farkas, J. B. Foresman, and D. J. Fox, Gaussian, Inc., Wallingford CT, 2016.

S2. S. Hirata, *Adv. Opt. Mater.*, 2017, **5**, 1700116.

S3. M. Brehm, B. Kirchner, *J. Chem. Inf. Model,* 2011, **51**, 2007–2023.

S4. D. Gurina, O. Surov, M. Voronova, A. Zakharov, *Nanomaterials,* 2020, **10**, 1256.

S5. M. Noorpour, A. Tarighat, *Ceram. Int.,* 2021, **47**, 19304–19314.

S6. R. Wang, J. Wang, T. Dong, G. Ouyang, *Constr. Build Mater.,* 2020, **240**, 117935.